

- D. Vodak, J. Wachter, M. O'Keeffe, O. M. Yaghi, *Science* **2002**, 295, 469.
- [4] P. S. Halasyamani, M. J. Drewitt, D. O'Hare, *Chem. Commun.* **1997**, 867; P. J. Hagraman, J. Zubietta, *Angew. Chem.* **1999**, 111, 2798; *Angew. Chem. Int. Ed.* **1999**, 38, 2634; S. A. Bourne, J. J. Lu, A. Mondal, B. Moulton, M. J. Zaworotko, *Angew. Chem.* **2001**, 113, 2171; *Angew. Chem. Int. Ed.* **2001**, 40, 2111; J. J. Lu, A. Mondal, B. Moulton, M. J. Zaworotko, *Angew. Chem.* **2001**, 113, 2174; *Angew. Chem. Int. Ed.* **2001**, 40, 2113.
- [5] J. Kim, B. L. Chen, T. M. Reineke, H. L. Li, M. Eddaoudi, D. B. Moler, M. O'Keeffe, O. M. Yaghi, *J. Am. Chem. Soc.* **2001**, 123, 8239; M. Eddaoudi, D. B. Moler, H. L. Li, B. L. Chen, T. M. Reineke, M. O'Keeffe, O. M. Yaghi, *Acc. Chem. Res.* **2001**, 34, 133.
- [6] R. Kitaura, K. Fujimoto, S.-I. Noro, M. Kondo, S. Kitagawa, *Angew. Chem.* **2002**, 114, 141; *Angew. Chem. Int. Ed.* **2002**, 41, 113; A. Escuer, R. Vicente, F. A. Mautner, M. A. S. Goher, M. A. M. Abu-Youssef, *Chem. Commun.* **2002**, 64; D. T. Vodak, M. E. Braun, J. Kim, M. Eddaoudi, O. M. Yaghi, *Chem. Commun.* **2001**, 2534.
- [7] a) Y.-B. Dong, M. D. Smith, H.-C. zur Loye, *Angew. Chem.* **2000**, 112, 4438; *Angew. Chem. Int. Ed.* **2000**, 39, 4271; b) R. J. Doedens, E. Yohannes, M. I. Khan, *Chem. Commun.* **2002**, 62; c) D. M. Ciurtin, M. D. Smith, H.-C. zur Loye, *Chem. Commun.* **2002**, 74.
- [8] Z. Shi, S.-H. Feng, S. Gao, L. -R. Zhang, G. Y. Yang, J. Hua, *Angew. Chem.* **2000**, 112, 2415; *Angew. Chem. Int. Ed.* **2000**, 39, 2325.
- [9] Y.-C. Liang, R. Cao, W.-P. Su, M.-C. Hong, W.-J. Zhang, *Angew. Chem.* **2000**, 112, 3442; *Angew. Chem. Int. Ed.* **2000**, 39, 3304; Y.-C. Liang, M.-C. Hong, W.-P. Su, R. -Cao, W.-J. Zhang, *Inorg. Chem.* **2001**, 40, 4574.
- [10] D. M. J. Doble, C. H. Benison, A. J. Blake, D. Fenske, M. S. Jackson, R. D. Kay, W.-S. Li, M. Schröder, *Angew. Chem.* **1999**, 111, 2042; *Angew. Chem. Int. Ed.* **1999**, 38, 1915; Y. Pei, P. Bergerat, O. Kahn, *J. Am. Chem. Soc.* **1994**, 116, 3866; E. Coronado, J.-R. Galán-Mascarós, C.-J. Gómez-García, J. Ensling, P. Gütllich, *Chem. Eur. J.* **2000**, 6, 552; E. Coronada, C.-J. Gómez-García, *Chem. Rev.* **1998**, 98, 273; R. Sieber, S. Decurtins, H. Stoeckli-Evans, C. Wilson, D. Yufit, J. A. K. Howard, S. C. Capelli, A. Hauser, *Chem. Eur. J.* **2000**, 6, 361; G. Ballester, E. Coronado, C. Giménez-Saiz, F. Romero, *Angew. Chem.* **2001**, 113, 814; *Angew. Chem. Int. Ed.* **2001**, 40, 792; E. Coronado, J. R. Galán-Mascarós, C. J. Gómez-García, J. M. Martínez-Agudo, *Inorg. Chem.* **2001**, 40, 113; F. Bellourard, M. Clemente-León, E. Coronado, J. R. Galán-Mascarós, C. J. Gómez-García, F. Romero, K. R. Dunbar, *Eur. J. Inorg. Chem.* **2002**, 1603.
- [11] B.-Q. Ma, S. Gao, G. Su, G.-X. Xu, *Angew. Chem.* **2001**, 113, 448; *Angew. Chem. Int. Ed.* **2001**, 40, 434.
- [12] J. M. Dominguez, F. Camara, J. M. Moreno, E. Colacio, H. Sroeckli, *Inorg. Chem.* **1998**, 37, 3046.
- [13] X-ray crystal structure analysis: The data were collected at 293(2) K on a CAD4 diffractometer (Mo $\alpha$  radiation;  $\lambda = 0.71073$  Å). The structure was solved by direct methods (SHELXTL Version 5.10) and refined by full-matrix least-squares on  $F^2$ . All non-hydrogen atoms were refined anisotropically. Crystal data for [C<sub>24</sub>H<sub>46</sub>Cu<sub>3</sub>Eu<sub>2</sub>N<sub>6</sub>O<sub>32</sub>]<sub>n</sub> (**1**): 0.50 × 0.40 × 0.40 mm, trigonal, space group  $P\bar{3}c1$  (no. 165),  $a = 13.4713(19)$ ,  $c = 14.922(3)$  Å,  $\gamma = 120^\circ$ ,  $V = 2345.3(7)$  Å<sup>3</sup>,  $Z = 2$ ,  $\rho_{\text{calcd}} = 1.958$  g cm<sup>-3</sup>,  $\mu(\text{MoK}\alpha) = 3.223$  mm<sup>-1</sup>,  $M_w = 1398.98$ . Of the 2615 reflections measured ( $2 < 2\theta < 56$ ), 1708 symmetry-independent reflections were used to solve the structure. Based on these data and 108 refined parameters,  $R_1 = 0.0410$  (all data),  $wR_2 = 0.0757$ , GOF ( $F^2$ ) = 1.111. Crystal data for [C<sub>24</sub>H<sub>46</sub>Cu<sub>3</sub>Nd<sub>2</sub>N<sub>6</sub>O<sub>32</sub>]<sub>n</sub> (**2**): 0.52 × 0.40 × 0.40 mm, trigonal, space group  $P\bar{3}c1$  (no. 165),  $a = 13.4027(19)$ ,  $c = 14.669(3)$  Å,  $\gamma = 120^\circ$ ,  $V = 2282.0(6)$  Å<sup>3</sup>,  $Z = 2$ ,  $\rho_{\text{calcd}} = 2.019$  g cm<sup>-3</sup>,  $\mu(\text{MoK}\alpha) = 3.699$  mm<sup>-1</sup>,  $M_w = 1409.64$ . Of the 1854 reflections measured ( $2 < 2\theta < 56$ ), 1189 symmetry-independent reflections were used to solve the structure. Based on these data and 114 refined parameters,  $R_1 = 0.0642$  (all data),  $wR_2 = 0.0870$ , and GOF ( $F^2$ ) = 1.011. Crystal data for [C<sub>24</sub>H<sub>46</sub>Cu<sub>3</sub>Eu<sub>2</sub>N<sub>6</sub>O<sub>32</sub>]<sub>n</sub> (**3**): 0.33 × 0.18 × 0.17 mm, trigonal, space group  $P\bar{3}c1$  (no. 165),  $a = 13.306(5)$ ,  $c = 14.528(5)$  Å,  $\gamma = 120^\circ$ ,  $V = 2227.6(14)$  Å<sup>3</sup>,  $Z = 2$ ,  $\rho_{\text{calcd}} = 2.101$  g cm<sup>-3</sup>,  $\mu(\text{MoK}\alpha) = 4.291$  mm<sup>-1</sup>,  $M_w = 1425.08$ . Of the 1533 reflections measured ( $2 < 2\theta < 56$ ), 1468 symmetry-independent reflections were used to solve the structure. Based on these data and 107 refined parameters,  $R_1 = 0.0497$  (all data),  $wR_2 = 0.1143$ , GOF ( $F^2$ ) = 1.127. Crystal data for [C<sub>24</sub>H<sub>38</sub>Cu<sub>3</sub>La<sub>2</sub>N<sub>6</sub>O<sub>29</sub>]<sub>n</sub> (**1a**): 0.32 × 0.24 × 0.22 mm, trigonal, space group  $P\bar{3}c1$  (no. 165),  $a = 13.5588(3)$ ,  $c = 14.9986(6)$  Å,  $\gamma = 120^\circ$ ,  $V = 2387.94(12)$  Å<sup>3</sup>,  $Z = 2$ ,  $\rho_{\text{calcd}} = 1.857$  g cm<sup>-3</sup>,  $\mu(\text{MoK}\alpha) = 3.157$  mm<sup>-1</sup>,  $M_w = 1344.98$ . Of the 9010 reflections measured ( $2 < 2\theta < 56$ ), 1721 symmetry-independent reflections were used to solve the structure. Based on these data and 100 refined parameters,  $R_1 = 0.1017$  (all data),  $wR_2 = 0.2352$ , GOF ( $F^2$ ) = 1.155. Crystal data for [C<sub>24</sub>H<sub>38</sub>Cu<sub>3</sub>Eu<sub>2</sub>N<sub>6</sub>O<sub>29</sub>]<sub>n</sub> (**3a**): 0.30 × 0.22 × 0.20 mm, trigonal, space group  $P\bar{3}c1$  (no. 165),  $a = 13.3031(2)$ ,  $c = 14.5660(3)$  Å,  $\gamma = 120^\circ$ ,  $V = 2232.42(7)$  Å<sup>3</sup>,  $Z = 2$ ,  $\rho_{\text{calcd}} = 2.025$  g cm<sup>-3</sup>,  $\mu(\text{MoK}\alpha) = 4.273$  mm<sup>-1</sup>,  $M_w = 1369.08$ . Of the 9618 reflections measured ( $2 < 2\theta < 48$ ), 1170 symmetry-independent reflections were used to solve the structure. Based on these data and 107 refined parameters,  $R_1 = 0.0359$  (all data),  $wR_2 = 0.0881$ , GOF ( $F^2$ ) = 1.091. CCDC-193487–193491 contains the supplementary crystallographic data for this paper. These data can be obtained free of charge via [www.ccdc.cam.ac.uk/conts/retrieving.html](http://www.ccdc.cam.ac.uk/conts/retrieving.html) (or from the Cambridge Crystallographic Data Centre, 12, Union Road, Cambridge CB2 1EZ, UK; fax: (+44)1223-336-033; or deposit @ccdc.cam.ac.uk).
- [14] Q.-D. Liu, S. Gao, J.-R. Li, Q.-Z. Zhou, K.-B. Yu, B.-Q. Ma, S.-W. Zhang, X.-X. Zhang, T.-Z. Jin, *Inorg. Chem.* **2000**, 39, 2488.

## Protein-Protein Interactions

### Design and Application of an $\alpha$ -Helix-Mimetic Scaffold Based on an Oligoamide-Foldamer Strategy: Antagonism of the Bak BH3/Bcl-xL Complex\*\*

Justin T. Ernst, Jorge Becerril, Hyung Soon Park, Hang Yin, and Andrew D. Hamilton\*

The design of low-molecular-weight ligands (< 750 Da) that recognize protein surfaces and subsequently disrupt protein-protein interactions is an area of intense research.<sup>[1]</sup> Current strategies for identifying small-molecule protein-surface antagonists primarily involve the use of combinatorial methods.

[\*] Prof. A. D. Hamilton, J. T. Ernst, J. Becerril, Dr. H. S. Park, H. Yin  
Department of Chemistry, Yale University  
P.O. Box 208107, New Haven, CT 06520-8107 (USA)  
Fax: (+1) 203-432-6144  
E-mail: [andrew.hamilton@yale.edu](mailto:andrew.hamilton@yale.edu)

[\*\*] We thank the National Institutes of Health for support of this work.

However, more recently, rational structure-based-design approaches have been presented.<sup>[1]</sup> Given the ubiquitous role of  $\alpha$  helices in mediating protein–protein interactions, we sought to explore the de novo design of scaffolds that present side-chain functionality with similar distance and angular constraints to that found along one face of an  $\alpha$ -helical secondary structure.<sup>[2]</sup> Herein we report a new class of proteomimetics based on a novel oligoamide foldamer; these structures serve as surface mimetics of the Bak BH3 domain. Analogues were identified by means of a fluorescence polarization assay and shown to bind Bcl-xL protein with low micromolar affinity and disrupt the Bak BH3/Bcl-xL complex.

The critical interactions for  $\alpha$ -helix recognition often involve the side chains of the  $i$ ,  $i+3$  and/or  $i+4$ , and  $i+7$  positions, which constitute one face of the helix. The goal of a designed helix mimetic is to provide a rigid preorganized framework from which functional groups are projected in such a way to resemble these key residues closely. Other criteria for mimetic design include a modular synthesis and moderate aqueous solubility.

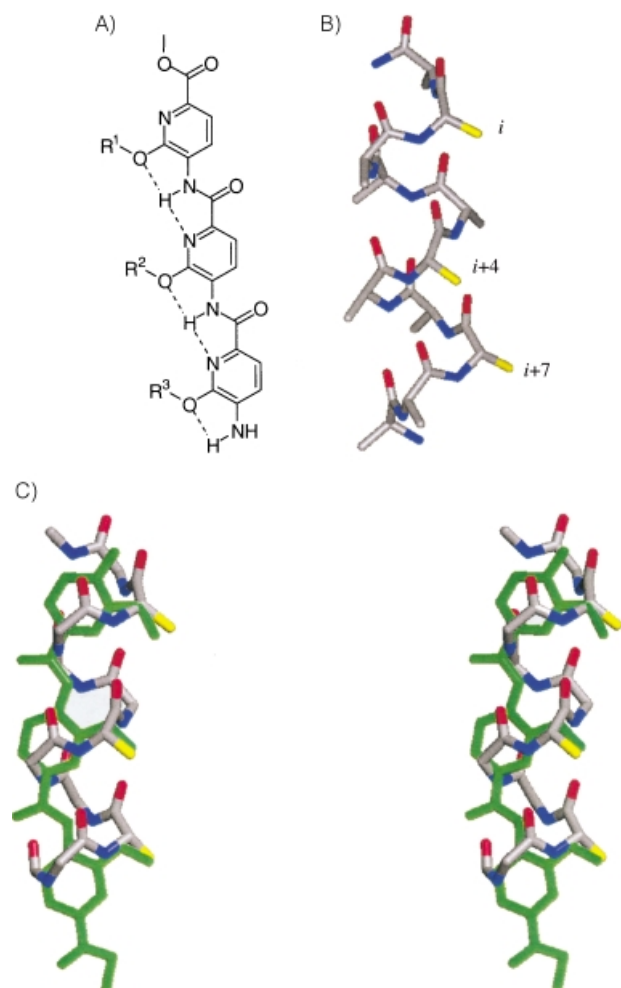


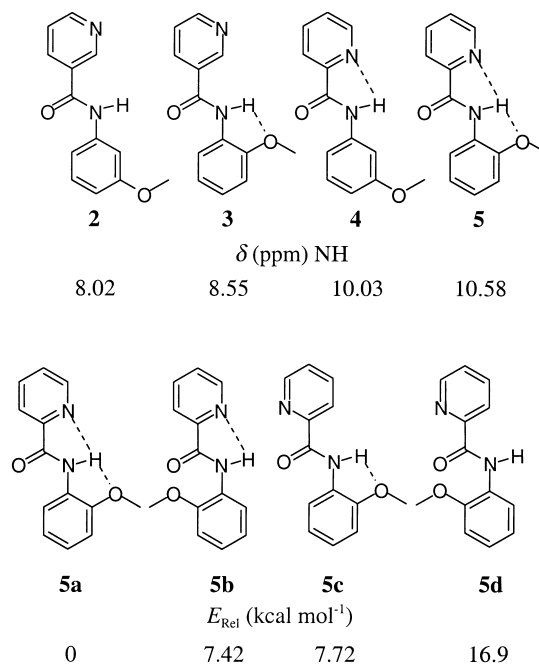
**Figure 1.** A) Structure of **1**. B) Polyaniline  $\alpha$ -helix (the  $i$ ,  $i+4$ , and  $i+7$  side chains are shown in yellow). C) Stereoview of the rms difference overlay of a polyaniline  $\alpha$ -helix ( $i$ ,  $i+4$ , and  $i+7$  positions) and **1a** (green).

A trispyridylamide scaffold **1** was designed as an  $\alpha$ -helix mimetic. The structure assumes a preferred conformation in which all three functional groups are projected on the same face of the molecule. This preorganization is accomplished through a stabilizing bifurcated hydrogen-bonding network as well as through the minimization of destabilizing alternative conformations (Figure 1 A).

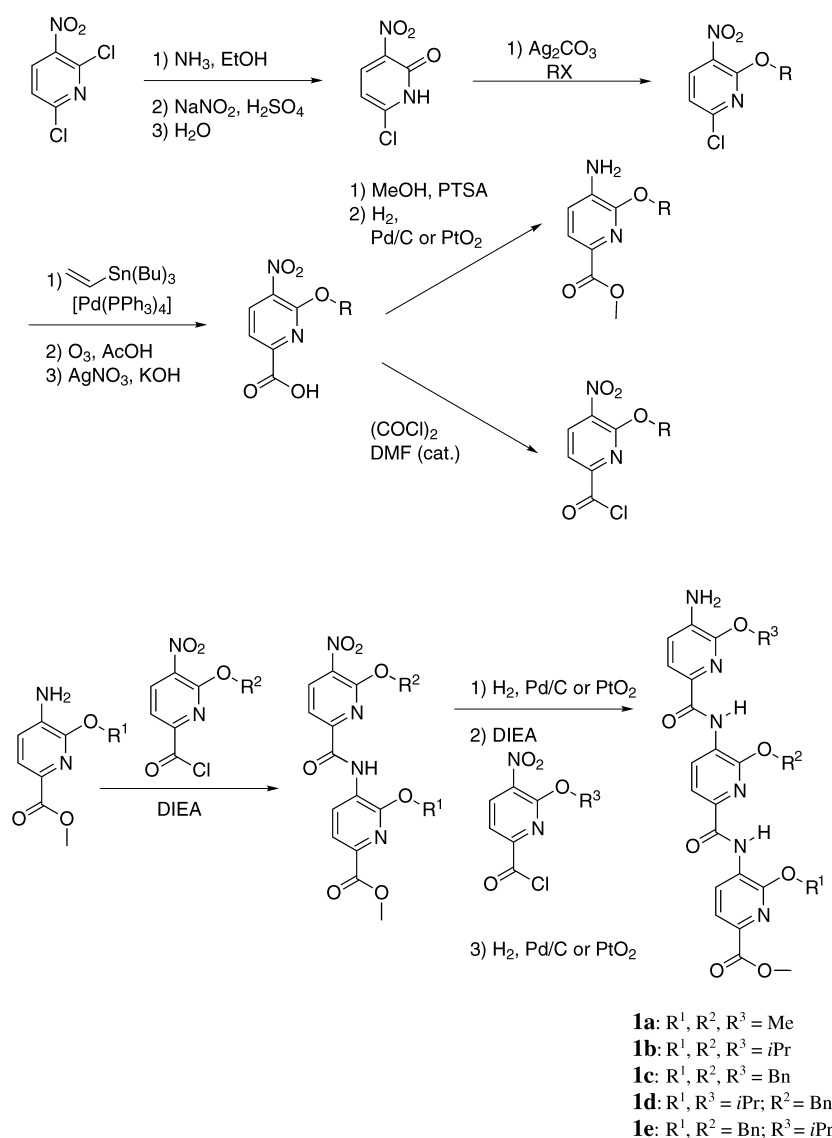
To probe this unique arrangement of noncovalent bonding, model systems **2–5** were synthesized and studied by means of  $^1\text{H}$  NMR spectroscopy (1 mM in  $\text{CDCl}_3$ ). The resonance for the amide hydrogen of **5** is concentration-independent and also shifted downfield relative to the corresponding NH signals of **3** and **4** ( $\delta = 8.55$  and  $10.03$  ppm, respectively), each containing one potential hydrogen bond, and **2** ( $\delta = 8.02$  ppm), which lacks hydrogen-bonding potential altogether (Scheme 1). Molecular-mechanics calculations (MM2) gave relative energies for the different planar conformations of **5** and these confirmed that **5a** is substantially preferred over **5b–5d**, which have unfavorable electrostatic interactions in addition to decreased hydrogen bonding.

MM2 energy minimization of **1a** ( $R_1, R_2, R_3 = \text{Me}$ ) showed the polyamide backbone to be quite planar. The alkoxy side chains, however, are rotated approximately  $45^\circ$  out of the plane of the carboxamide backbone, presumably to optimize the position of the lone pairs of electrons on the oxygen atom of the ether functionalities for hydrogen bonding. Overlaying the  $\alpha$  and  $\beta$  positions of the  $i$ ,  $i+4$ , and  $i+7$  alanine methyl groups of an  $\alpha$  helix (Figure 1 B) with the corresponding side-chain atoms of a low-energy conformation of **1a** shows close correspondence of the two structures (Figure 1 C, root-mean-square deviation =  $0.94 \text{ \AA}$ ).

The modular synthesis of derivatives of **1** (**1a–1e**) is shown in Scheme 2. The different monomers can be easily



**Scheme 1.** Analogues of **1** used in model studies.



**Scheme 2.** Synthesis of derivatives of **1**. DIEA = diisopropylethylamine.

prepared through *O*-alkylation of 6-chloro-3-nitro-2(1*H*)-pyridone with the desired electrophile.<sup>[3]</sup> Assembly of the pyridyl trimers is accomplished through iterative amide bond formation between the aryl amines and aryl acid chlorides by using standard coupling conditions.

An X-ray crystal structure of nitro derivative **6** shows that the polyamide backbone is indeed planar and that the molecule adopts the expected conformation in which all the isopropoxy side chains are projected from one side of the molecule (Figure 2). The distances between the amide hydrogen atoms and the pyridine nitrogen atoms (2.1 Å) and the oxygen atoms of the side chains (2.2 Å) are consistent with the formation of four five-membered hydrogen-bonding rings within the structure. The torsional angles of the alkoxy side chains in the solid state are 4°, 0°, and 15° out of the plane of the aromatic backbone. Although these angles are less than that predicted by

computational analysis, it is assumed that the side chains will be more flexible in solution.

NOESY <sup>1</sup>H NMR spectroscopy experiments (20 mm in  $\text{CDCl}_3$ ) were conducted to probe the conformation of **6** in solution. Cross peaks were observed between the amide protons and the methine and methyl protons of the isopropoxy side chains. However, no cross peaks were observed between the amide protons and the pyridine 4-protons. Furthermore, variable-temperature <sup>1</sup>H NMR spectroscopy experiments from 20 to 125 °C using **1b** (1 mm in  $\text{CD}_2\text{Cl}_2$ ) revealed only a 0.12 ppm upfield shift for the signal from the amide protons. Repeating the experiment in  $[\text{D}_6]\text{DMSO}$  also resulted in only a slight upfield shift ( $\Delta\delta = -0.95$  ppm). These results suggest that the backbone conformation in which all the alkoxy groups project from the same face of the molecule is adopted, even in a polar solvent. The presence of NOE cross peaks between the side-chain methyl groups and the backbone amide hydrogen atoms suggests that the side chains have some flexibility, enabling the structure to adopt the desired conformations for  $\alpha$ -helix mimicry (Figure 1).

To test the trispyridylamides as proteo-mimetic scaffolds, we studied the complex formed between the BH3 domain of the proapoptotic protein Bak and the antiapoptotic protein Bcl-xL.<sup>[4]</sup> Bak and Bcl-xL belong to the Bcl-2 family of proteins, which regulates cell death through an intricate balance of homodimer and heterodimer complexes formed within this class of proteins.<sup>[5]</sup> Overexpression of antiapoptotic proteins such as Bcl-xL and Bcl-2

prevent cells from triggering programmed death pathways and has been linked to a variety of cancers.<sup>[5c]</sup> A current strategy for developing new anticancer agents is to identify

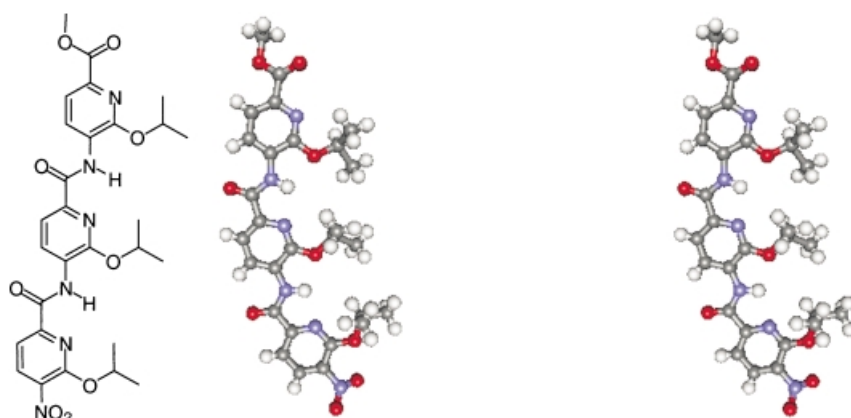


**Figure 2.** Crystal structure of **6**.

molecules that bind to the Bak-recognition site on Bcl-xL, disrupting the complexation of the two proteins and therefore antagonizing Bcl-xL function.<sup>[2a]</sup> To date, there have been several reports of small molecules, identified from screening large libraries, that disrupt the Bak BH3/Bcl-xL complex, with the best inhibitors having  $K_i$  values in the low micromolar range.<sup>[6]</sup>

The structure determined by NMR spectroscopy<sup>[4]</sup> shows the 16 residue BH3 domain peptide from Bak (aa 72 to 87,  $K_d \approx 300$  nM) bound in a helical conformation to a hydrophobic cleft on the surface of Bcl-xL, formed by the BH1, BH2, and BH3 domains of the protein. The crucial residues for binding were shown by alanine scanning to be V74, L78, I81, and I85,<sup>[4]</sup> which project in an  $i, i+4, i+7, i+11$  arrangement from one face of the  $\alpha$ -helix. The Bak peptide is a random coil in solution but adopts an  $\alpha$ -helical conformation when complexed to Bcl-xL. Studies utilizing stabilized helices of the Bak BH3 domain have shown the importance of this conformation for tight binding.<sup>[7]</sup>

Molecule **1b** represented our initial design for a Bcl-xL antagonist in which the isopropoxy side chains serve to mimic the key hydrophobic residues of the Bak BH3 domain. Analogues **1a**, and **1c–1e** were also prepared to probe the degree of hydrophobicity of the scaffold side chains (Scheme 2). The BH3 domain of another proapoptotic Bcl-2 family member (Bad) has larger hydrophobic groups at these positions (Tyr, Phe) and binds with a higher affinity than Bak to Bcl-xL.<sup>[8]</sup>

To study the ability of **1a–1e** to bind Bcl-xL and disrupt the Bak BH3/Bcl-xL complex, we employed a previously reported fluorescence polarization assay.<sup>[8d]</sup> Displacement of a fluorescein-labeled Bak BH3 peptide from the Bcl-xL complex by competitive binding of a small molecule will lead to a reduction in polarization. Taking into account the known binding affinity of the Bak peptide, the change in polarization can be used to calculate the binding affinity of the inhibitor. Using this assay, compounds **1b**, **1d**, and **1e** (Scheme 2) were found to inhibit the Bak BH3/Bcl-xL complex successfully, binding to Bcl-xL with low micromolar affinity ( $K_i$  values of 2.3, 9.8, and 1.6  $\mu$ M, respectively).<sup>[9]</sup> Molecule **1c** (Scheme 2), which contains three benzyloxy side chains, showed reduced affinity ( $K_i > 20$   $\mu$ M) for the hydrophobic pocket of Bcl-xL. Finally, the trimethoxy derivative **1a** as well as the isopropoxy dimer **7** (Scheme 3) showed no observed binding below a concentration of 25  $\mu$ M.

To probe the mode of binding of **1b**, molecular-docking studies were completed using the structure of Bcl-xL present in the Bak BH3/Bcl-xL complex. The conformational flexibility of the side chains in **1b** was taken into account and the different binding modes were ranked using an energy-scoring function. The results of this study suggest that molecule **1b** binds into the same hydrophobic cavity as Bak (Figure 3).

The initial success of trimer **1b** suggested that extending the design to include four isopropoxy subunits would improve binding, since the tetramer **8** (Scheme 3) would have the potential to mimic all the key hydrophobic residues of Bak used for binding (V74, L78, I81, I85). Computational docking studies suggested that the preferred mode of binding of **8** is in the hydrophobic pocket with the isopropoxy side chains

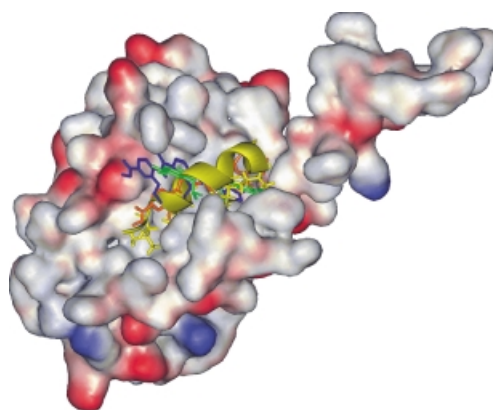
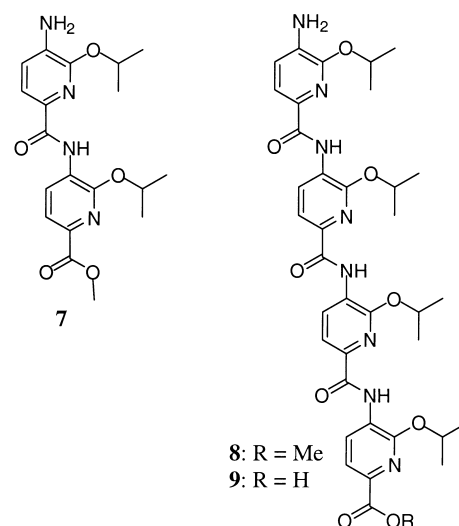


**Figure 3.** Results of the molecular-docking studies of **1b** and Bcl-xL. The three highest-ranked binding modes are shown: green (rank 1), orange (rank 2), and blue (rank 3). The Bak BH3 peptide (yellow) is overlaid with the docked structures. The key hydrophobic side chains of Bak are shown as stick representations (V74, L78, I81, I85).



**Scheme 3.** Dimeric (**7**) and tetrameric (**8**, **9**) analogues of **1**.

having an analogous spatial arrangement to the four key alkyl side chains of Bak. Unfortunately, **8** proved to be insoluble under the experimental conditions of the fluorescence polarization assay. To improve the aqueous solubility of this system, the methyl ester was hydrolyzed to yield the free acid derivative **9**. Although compound **9** mimics all four key hydrophobic side chains of Bak, it shows a slightly lower affinity ( $K_i = 4.17$   $\mu$ M) for Bcl-xL than does trimer **1b**.

In summary, a new scaffold for mimicking the surface functionality of an  $\alpha$  helix was designed using a novel polyamide foldamer. The mimetic strategy was applied to the synthesis of antagonists of the Bak BH3/Bcl-xL complex. Results from fluorescence polarization experiments suggest that three trimer analogues (**1b**, **1d**, and **1e**) have a low micromolar affinity for Bcl-xL and inhibit its interaction with Bak. Extension of the design to include four pyridyl subunits (i.e. **9**) failed to improve the binding affinity of the mimetic

system. Molecular-docking studies suggest that the inhibitors bind into the Bak-recognition site on the surface of Bcl-xL.

Received: May 21, 2002

Revised: October 22, 2002 [Z19346]

- [1] a) P. L. Toogood, *J. Med. Chem.* **2002**, *45*, 1–16; b) A. G. Cochran, *Curr. Opin. Chem. Biol.* **2001**, *5*, 654–659.
- [2] For examples of  $\alpha$ -helix mimetics, see: a) O. Kutzki, H. S. Park, J. T. Ernst, B. P. Orner, H. Yin, A. D. Hamilton, *J. Am. Chem. Soc.* **2002**, *124*, 11 832–11 839; b) J. T. Ernst, O. Kutzki, A. K. Debnath, S. Jiang, H. Lu, A. D. Hamilton, *Angew. Chem.* **2002**, *114*, 288–291; *Angew. Chem. Int. Ed.* **2002**, *41*, 278–281; c) B. P. Orner, J. T. Ernst, A. D. Hamilton, *J. Am. Chem. Soc.* **2001**, *123*, 5382–5383; d) H. Xuereb, M. Maletic, J. Gildersleeve, I. Pelczer, D. Kahne, *J. Am. Chem. Soc.* **2000**, *122*, 1883–1890; e) W. P. Nolan, G. S. Ratcliffe, D. C. Rees, *Tetrahedron Lett.* **1992**, *33*, 6879–6882.
- [3] G. C. Hopkins, J. P. Jonak, H. J. Minnemeyer, H. Tieckelmann, *J. Org. Chem.* **1967**, *32*, 4040–4044.
- [4] M. Sattler, H. Liang, D. Nettesheim, R. P. Meadows, J. E. Harlin, M. Eberstadt, H. S. Yoon, S. B. Shuker, B. S. Chang, A. J. Minn, C. B. Thompson, S. W. Fesik, *Science* **1997**, *275*, 983–986.
- [5] a) M. C. Raff, *Science* **1994**, *264*, 668–669; b) D. T. Chao, S. J. Korsmeyer, *Annu. Rev. Immunol.* **1998**, *16*, 395–419; c) C. B. Thompson, *Science* **1995**, *267*, 1456–1462; d) L. L. Rubin, K. L. Philpott, S. F. Brooks, *Curr. Biol.* **1993**, *3*, 391–394.
- [6] a) I. J. Enyedy, Y. Ling, K. Nacro, Y. Tomita, X. Wu, Y. Cao, R. Guo, B. Li, X. Zhu, Y. Huang, Y.-Q. Long, P. P. Roller, D. Yang, S. Wang, *J. Med. Chem.* **2001**, *44*, 4313–4324; b) A. Degterev, A. Lugovskoy, M. Cardone, B. Mulley, G. Wagner, T. Mitchison, J. Yuan, *Nat. Cell Biol.* **2001**, *3*, 173–182; c) S.-P. Tzung, K. M. Kim, G. Basanez, C. D. Giedt, J. Simon, J. Zimmerberg, K. Y. J. Zhang, D. M. Hockenbery, *Nat. Cell Biol.* **2001**, *3*, 183–191; d) J.-L. Wang, D. Liu, Z.-J. Zhang, S. Shan, X. Han, S. M. Srinivasula, C. M. Croce, E. S. Alnemri, Z. Huang, *Proc. Natl. Acad. Sci. USA* **2000**, *97*, 7124–7129.
- [7] J. W. Chin, A. Schepartz, *Angew. Chem.* **2001**, *113*, 3922–3925; *Angew. Chem. Int. Ed.* **2001**, *40*, 3806–3809.
- [8] A. M. Petros, D. G. Nettesheim, Y. Wang, E. T. Olejniczak, R. P. Meadows, J. Mack, K. Swift, E. D. Matayoshi, H. Zhang, C. B. Thompson, S. W. Fesik, *Protein Sci.* **2000**, *9*, 2528–2534; b) A. Kelekar, B. S. Chang, J. E. Harlan, S. W. Fesik, C. B. Thompson, *Mol. Cell. Biol.* **1997**, *17*, 7040–7046.
- [9] The protein-binding experiments were carried out by diluting a solution of the helix mimetic in DMSO into an aqueous buffer solution (25°, 10 mM PBS, pH 7.4) of Bcl-xL and the fluorescently labeled Bak peptide.

## Theory of Pyramidal Boron

### Stabilization of Tricoordinate Pyramidal Boron: Theoretical Studies on $\text{BSiH}_5$ , $\text{BSi}_2\text{H}_5$ , $\text{C}\text{BGeH}_5$ , and $\text{CBSnH}_5^{**}$

Kalathingal T. Giju, Ashwini Kumar Phukan, and Eluvathingal D. Jemmis\*

The dramatic computational discoveries<sup>[1]</sup> and experimental realizations<sup>[2]</sup> of planar tetracoordinate carbon and planar tetracoordinate boron<sup>[3]</sup> species have set the stage for other rule-breaking structures. Preference for the trigonal planar arrangement in carbenium ions and tricoordinate boron species is one of the tenets of main-group chemistry that remains unchallenged. An unconstrained pyramidal carbenium ion or its boron equivalent has, so far, remained elusive. We report here, for the first time, the computational<sup>[4]</sup> discovery of a neutral-ground-state molecule, silaborirane **1**, which contains a tricoordinate pyramidal boron center. The conventional planar geometry **2** is a transition state with the imaginary frequency corresponding to pyramidalization around the boron atom. Similar results are obtained when the Si atom in **1** is replaced by Ge and Sn.

Structure **1** is derived from the  $\text{C}_{2v}$  cyclopropyl cation **3**, which is calculated to be a transition state.<sup>[5a,b]</sup> Replacement of  $\{\text{CH}\}^+$  by  $\{\text{BH}\}$  leads to borirane **4**, which is a minimum with a trigonal planar boron center.<sup>[5c]</sup> Replacement of one  $\text{CH}_2$  group by an  $\text{SiH}_2$  group yields a three-membered ring comprised of three different atoms. Its conventional structure (**2**), with a planar tricoordinate boron atom, is calculated to be a transition state with an imaginary frequency ( $331.4\text{ cm}^{-1}$  at B3LYP/6-311 + G\*\*);<sup>[6]</sup> this leads to the minimum-energy structure **1** with a pyramidal arrangement at the boron center, which is lower in energy by  $2.4\text{ kcal mol}^{-1}$ . This energy difference increases to  $4.1\text{ kcal mol}^{-1}$  at the CCSD(T)/6-311 + G\*\* level of theory.<sup>[7–9]</sup>

Pyramidalization at the boron center causes substantial changes in the structure (Figure 1). In order to understand these changes, the structures **1** and **2** are visualized from different perspectives. While there is very little change in the H-Si-H and H-C-H angles of **1** and **2**, the H-Si-C and H-C-Si angles change on the transition from **2** to **1**, which is indicative of an unusual twisting of the  $\text{CH}_2$  and  $\text{SiH}_2$  groups with respect to each other (Table 1).

By symmetry, the pairs of angles H-Si-C ( $116.8^\circ$ ), H-C-Si ( $119.7^\circ$ ), and H-Si-B ( $122.2^\circ$ ) are the same in **2**. However in **1**,

[\*] Prof. Dr. E. D. Jemmis, Dr. K. T. Giju, A. K. Phukan  
School of Chemistry  
University of Hyderabad  
Hyderabad – 500 046 (India)  
Fax: (+91) 40-301-2460  
E-mail: jemmis@uohyd.ernet.in

[\*\*] This work was supported by the Board of Research in Nuclear Sciences, Mumbai, Department of Science and Technology, and the University with Potential for Excellence Program of the University Grants Commission, New Delhi, India. A.K.P. thanks CSIR for a Senior Research Fellowship.